Evaluation of zirconia modification on the durability of natural fiber-reinforced cement composites using accelerated aging

Helong Song [a,*], Tao Liu [b], Florent Gauvin [a], H.J.H. Brouwers [a]

[a] Department of the Built Environment, Eindhoven University of Technology, P.O. Box 513, 5600, MB, Eindhoven, the Netherlands
[b] Department of Environmental and Resource Engineering, Technical University of Denmark, Brovej 118, Lyngby, Denmark

ARTICLE INFO

ABSTRACT

In this research, the main target focuses on accelerating aging tests for the evaluation of durability performance on ZrO_2-modified fiber-reinforced cement composites. Then, the study focuses on the comparison between two alkali-resistance behaviors (i.e. alkali hydrolysis and mineralization) of unmodified and ZrO_2-modified fibers in various controlled alkali solutions. For such purposes, the mechanical strengths of the composites under accelerating aging were measured. The thermal stability of embedded fibers, the evolution of hydration products on the fiber surfaces, and the interface compatibility were also studied to understand the mechanism behind the potential enhancement of durability. Besides, the alkali resistance of fibers was investigated by measuring the tensile strength loss. Results show that the composites reinforced with ZrO_2-modified fibers retain their high mechanical strength, even when subjected to long-term wetting-drying cycles. Moreover, ZrO_2 modification can significantly reduce or even prevent the precipitation of portlandite and ettringite on the surfaces of the embedded fibers. According to alkali resistance tests, fibers with ZrO_2 film exhibited superior resistance. The results of the durability of NFRCCs under accelerated aging conditions accelerate their practical application in outdoor building projects.

1. Introduction

Due to their excellent flexural behavior, extensive research has been conducted on fiber-reinforced building composites, such as fiber-reinforced cement-based composites [1] and fiber-reinforced geopolymer composites [2]. In recent years, there has been a growing interest in natural fiber-reinforced building composites, particularly in reinforced cement composites [3], driven by global sustainability demands, cost-effectiveness, and widespread availability.

Currently, natural fiber-reinforced cement composites (NFRCCs) are being actively explored for applications in the civil engineering and building fields (Table 1), specifically for applications in the field of low-cost housing [4–6]. However, the poor durability of NFRCCs, attributed to the alkaline hydrolysis and the mineralization of the embedded natural fiber, greatly limits their practical application.

To address this problem, Two strategies have been widely employed to increase long-term durability, namely (1) modification of the cementitious matrix [12,13] and (2) fiber treatment [14]. The second approach has been widely adopted due to the additional advantage of optimizing the fiber-matrix interface. Therefore, this study is also focused on fiber treatment. In terms of fiber treatment used in NFRCCs, there are various methods including thermal treatment [15], alkali treatment [16], and physical-chemical

---

impregnation [17,18] among others. Especially, the introduction of functional substances through dipping into natural fibers has been deemed as an effective and low-cost route to improve the durability of NFRCCs by preventing the attack on NF from the alkaline pore solution. For example, Canovas et al. [19] enhanced the durability of Portland cement mortars reinforced with sisal fibers by coating timber extracts (e.g. colophony, tannin, and vegetable oil) onto sisal fibers and the flexural strength results of the composites showed that mortars reinforced with impregnated fibers exhibited better durability. Bilba and his co-worker [20] used an emulsion of silane to coat bagasse fibers for reinforcement of cementitious composites, which concluded that 6 % weight of silane is capable of reducing the water absorption potential of fibers, hence increasing the durability. Although these treatment methods can prolong the durability of NFRCCs a certain, some new problems such as the high cost and complicated treatments are introduced.

Given that zirconium dioxide (ZrO_2) has been successfully applied on glass fibers, which is known as alkali-resistance (AR) glass fibers, to improve their durability in cement matrix [18,21], several researchers have used zirconium dioxide (ZrO_2) on natural fiber modification to improve the durability of the fiber-reinforced cement composites [21,22], and it was reported that ZrO_2-treated yarn fibers can effectively prolonger the durability of reinforced cement composites at room conditions [18]. However, the durability of NFRCCs under harsh environments has yet to be performed. In addition, the alkali resistance behaviors (alkali hydrolysis and mineralization) of ZrO_2 on natural fiber were not fully unclear.

Hence, the goal of this study is to evaluate the durability of ZrO_2-modified fiber-reinforced cement composites under harsh conditions and reveal the related mechanism. In this study, hemp fiber is selected as the research objective considering the overabundant waste of hemp fibers produced annually in Europe [23]. The ZrO_2 sol was employed to modify hemp fibers by dipping method. Subsequently, hemp fiber-reinforced cement composites (HFRCCs) were obtained by randomly mixing short fibers with cement-based materials. To assess the durability of the composites under harsh conditions, the mechanical strength of the composites was tested at different wetting-drying cycles. Meanwhile, to fully understand the mechanism, the property performances of the embedded fibers were characterized by the thermogravimetric measurement and the element components tests on hydration products of fiber surfaces. Furthermore, to compare the performance of ZrO_2 in terms of its resistance to alkali hydrolysis and resistance to mineralization, the tensile strengths of the fibers exposed in different designed alkali solutions were investigated. The outcomes of this study can provide the theoretical guidance to accelerate the industrial application of the NFRCCs (HFRCCs) such as pavement blocks and low-cost housing.

2. Experiments

The durability of HFRCCs under accelerated aging conditions is assessed by analyzing the properties of embedded fibers, the mechanical strength of entire HFRCCs, and fiber-matrix compatibility, as illustrated in Fig. 1. The alkali resistance behaviors of fibers under different alkali mediums were compared to further evaluate the fiber surface treatment on the durability of entire composites.

2.1. Raw materials

Technical hemp fibers were supplied by HempFlax Group B.V. (The Netherlands). All the chemical components used for the pretreatment and the preparation of the ZrO_2 Sol like zirconyl chloride octahydrate ($ZrOCl_2 \cdot 8H_2O$), Polyethylene glycol (PEG400), Hydrogen peroxide (30 wt%) and absolute alcohol were purchased from the VWR®, part of Avantor. The commercial ordinary Portland cement (OPC) CEM I was provided by ENCI B.V, (The Netherlands).

2.2. Methods

2.2.1. Fiber treatment

Prior to the experiment, some long hemp fibers were washed and cut (length = 12 cm) for the single fiber tensile testing, which will be specifically described in the following section. The remaining shorter fibers were cut (length ≈ 2 cm) for the preparation of fiber-cement composites. Subsequently, these fibers were pretreated with both acetone and diluted alkaline solution to remove the impurities on the fiber surface (i.e. pectin, lignin, and hemicellulose). This step was detailed in the previous work.

The method used to prepare the ZrO_2 sol follows the work of Wang et al. [24]: The ZrO_2 sol was prepared and aged for 1 day for coating. The pretreated fibers were completely immersed in the ZrO_2 sol for 5 min, filtered twice, and dried at 70 °C for 1 day. A ZrO_2 layer was formed on the fiber surface. The treatment process is schematically shown in Fig. 2.

Table 1
Summary of the effect of different natural fibers on the flexural strength of NFRCCs.

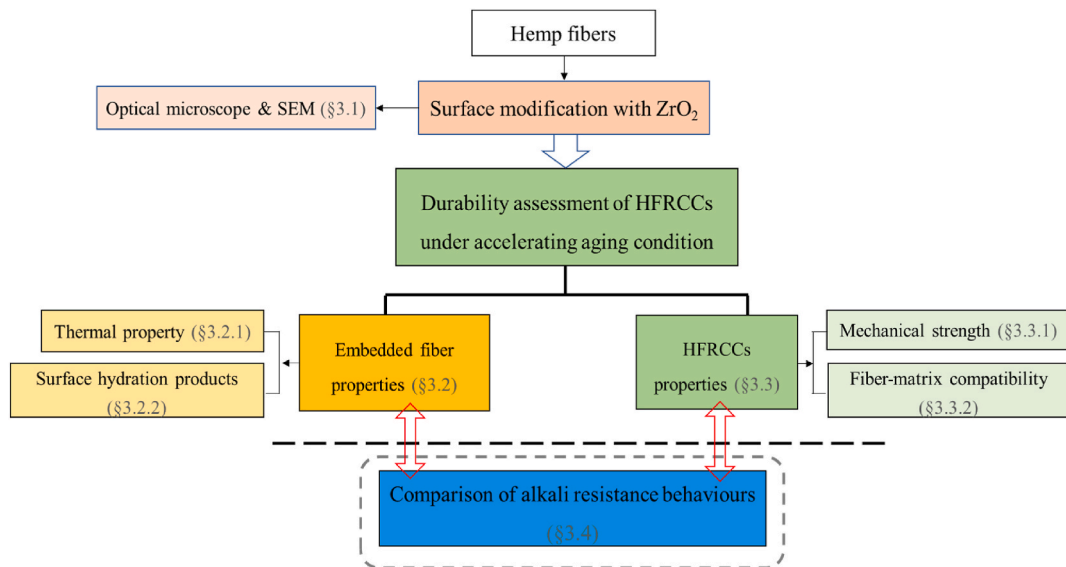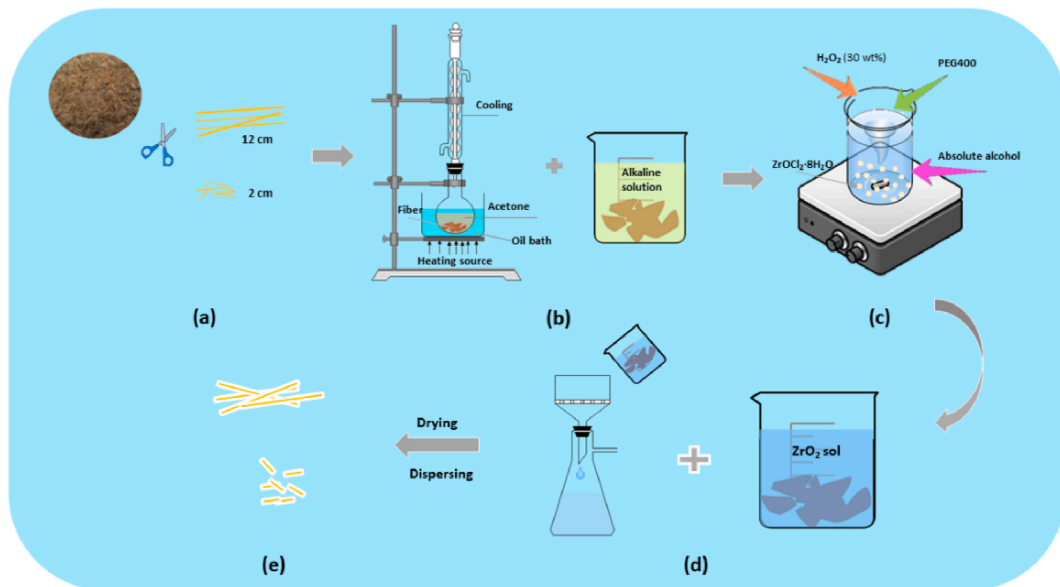| Natural fibers	Fiber content (%)	Composite type	Flexural strength (MPa)		Ref.
			Control	With fibers	
Kenaf fibers	1.0–2.0 %	Mortars	5.1–7.5	7.4–11.0	[7]
Jute fibers	1.5	Mortars	4.9	5.7	[8]
Coconut fibers	1.5	Mortars	4.9	6.1	[8]
Kelp fiber	1.5	Mortars	4.9	6.3	[8]
Flax fibers	2.0	Mortars	6.3	7.1–9.5	[9]
Hemp fibers	1.0–3.0	Mortars	5.0	5.1–5.9	[10]
Hemp fibers	1.0	Mortars	6.8	7.5–8.1	[11]

Fig. 1. Overview of this work.

Fig. 2. Schematic illustration for the process of the pretreatment and ZrO$_2$ modification on fibers. (a) Cutting raw fibers. (b) fibers pretreating. (c) Preparing ZrO$_2$ sol. (d) fibers immersed and filtered. (e) ZrO$_2$ coated on fibers.

2.2.2. Fiber composites preparation

HFRCCs with 2 % (by weight, relative to cement weight) were prepared from original, pretreated, and ZrO$_2$-treated fibers. The hemp fibers used were around 2 cm in length, and their distribution in the composites was random orientation. The sand-cement ratio and water-cement ratio used in this work were 3 and 0.5, respectively. The main purpose of sand addition is to ensure the fibers randomly disperse. In addition to that, the short fibers were also distributed by hand followed by mixing continued at middle speed for 2 min to disperse uniformly. The flowability of all mortars was adjusted and kept around 18 mm using a polycarboxylic ether-based superplasticizer, which is to avoid the influence of the absorbing water of fiber on the water-cement ratio. The specimens were demolded after 24 h and kept in a climatic chamber at 20 ± 2 °C and 50 ± 5 % humidity for 28 days.

After that, the mortar specimens were subjected to wetting-drying cycles to accelerate aging. The wetting-drying cycling approach in our study was adopted based on Ref [25]. In detail, one cycle includes the wetting step (submerged in sealed tap water at room temperature for 7 days), the drying step (dried in a circulating air environment at 60 °C for 4 days), and the cooling step (cooled down at room temperature for 3 h). Finally, the investigated specimens were repeatedly exposed to different cycles for the later tests.

2.3. Alkali resistance test

The deterioration of untreated, pretreated, and ZrO$_2$-treated long fibers exposed to different alkali environments gave important information concerning the durability of fiber-cement mixture specimens. The degradation of the fibers was measured as strength loss occurred over time, for different treated fibers under three kinds of environments: fibers stored in water; fibers stored in a saturated solution of calcium hydroxide of pH 12.6; and fibers stored in a solution of sodium hydroxide of pH 12.6. These fibers were stored in small containers with tap water or chemical solutions for up to 90 days, as is shown in Fig. 3. The container was covered and the pH of the solutions was checked at regular intervals; solutions that had not retained the initial pH value were replaced. In addition, considering the security risk of the Lab room, the fog equipment is turned on and set for 6 h every day. After different storing days, the fibers were dried in the oven at 60 °C for 24 h and then tensile tested.

2.4. Characterization

The effect of fiber modification was characterized by a Zeiss optical microscope and a Phenom pro-X scanning electron microscopy (SEM). The thermogravimetric analysis (TGA, NETZSCH STA 449 F1) was performed on both unembedded fibers and the extracted fibers from the cementitious matrix to evaluate the thermal behavior of these fiber samples. The temperature was set between 50 °C and 700 °C and the environment was in a nitrogen flow of 100 mL/min at a heating rate of 20 °C/min. The isothermal calorimeter (TAM air, Thermometric) is employed to study the interfacial compatibility between the fibers and the cement. In the sample preparation, we thoroughly shook and mixed the fibers and dried powders homogeneously. This was done to ensure the uniform dispersion of fibers in the fresh slurry, all while shortening the stirring time after adding water to enhance the accuracy of the tested results. The compressive strength and flexural strength of NFRCCs in this work were conducted following EN 196-1 [26]. The tests were repeated three times. Besides, the tensile strength of long fibers was determined using the EZ 20 Lloyd Instrument (AMETEK) testing machine with a maximum capacity of 100 N. The load was applied at a constant rate of about 0.2 mm/min. The tests were carried out after 0, 12 d, 30 d, and 90 d of immersion in the two solutions or the water. For each test, three different treated fiber samples (untreated, pretreated, and ZrO$_2$-treated) were prepared, with the tests being replicated ten times.

3. Results

3.1. Fiber surface modification

The fibers, subjected to various treatments including untreated, only pretreatment, and both pretreatment and ZrO$_2$ coating, exhibit distinct differences in both colors and surface morphology, as illustrated in Fig. 4.

In Fig. 4(a), optical and corresponding SEM images of raw hemp fibers are presented. The fiber surface is observed to have a dark yellow color, attributed to non-cellulosic substances such as pectin and lignin, as confirmed by IR-spectroscopy [27]. Meanwhile, a smooth surface was observed from the corresponding SEM image. After the alkali-acetone pretreatment, the color of the fiber surface became brighter, more microfibril fibers appeared and the surface became rough relief as illustrated in Fig. 4(b). These phenomena can be explained by the removal of some non-cellulosic substances under the pretreatment process. To be more specific, some impurities (i. e. wax and pectin) of fiber surfaces were removed by the acetone extraction procedure [28]. Furthermore, sodium hydroxide was employed to remove the other impurities (i.e. lignin, pectin, and hemicellulose) in the first layer of the fiber cell wall [29]. In addition, the rough surface of the pre-treated fiber is more beneficial for the physical attachment of following ZrO$_2$. As seen in Fig. 4 (c), a unique modified layer of ZrO$_2$ was coated on the pre-treated fibers which could resist the alkaline attack and degradation from the cement matrix [30]. Also, the surface became quite rough, which could benefit the increase of the interface bonding between fibers and the cement matrix [31].

3.2. Effect of ZrO$_2$ modification on the properties of embedded fibers

To better understand the actual degradation evolution of different treated hemp fibers embedded in the cementitious matrix throughout normal curing time and accelerated aging, thermogravimetric analysis (TGA) was performed on embedded fibers, and
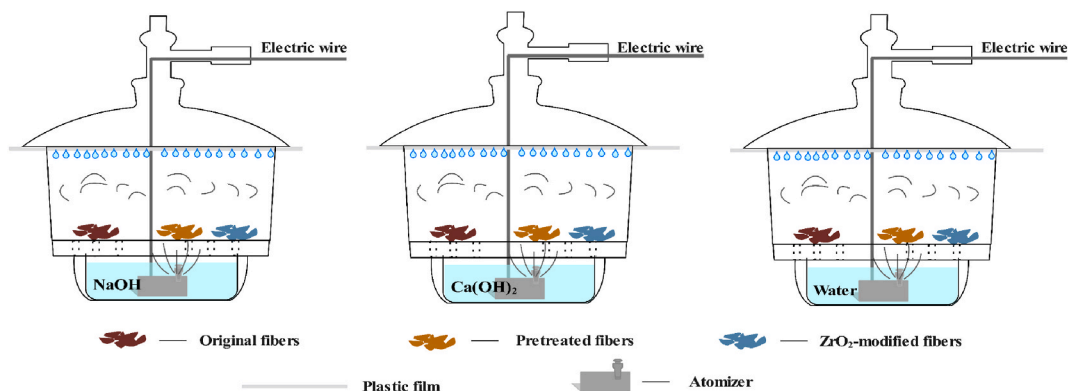

Fig. 3. Schematic illustration for different treated fibers processed in three types of environments: NaOH solution, saturation Ca(OH)$_2$ solution, and water.
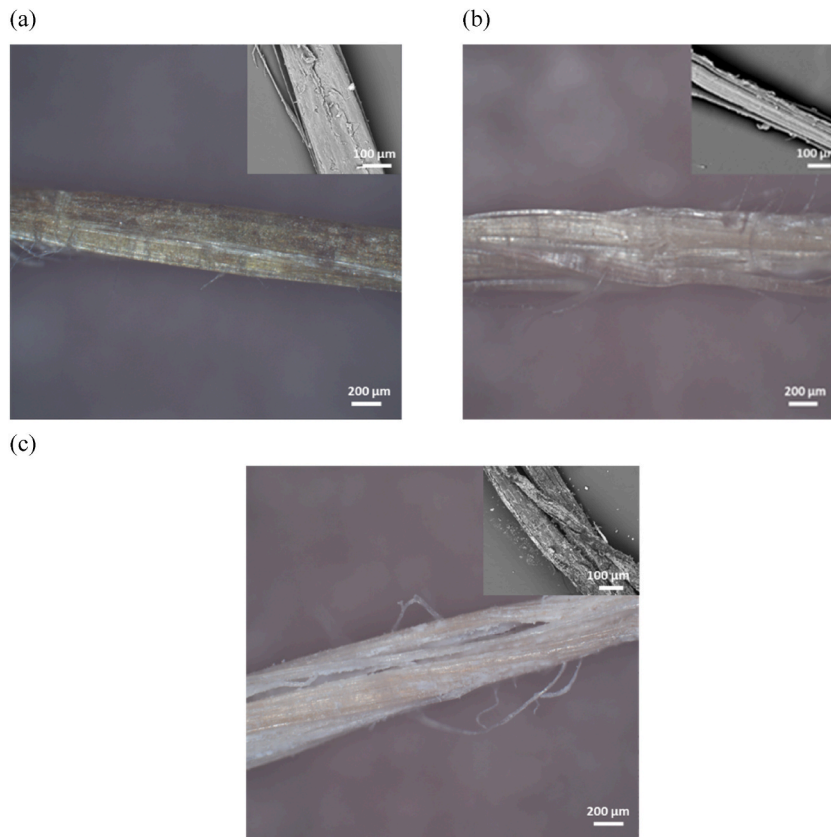
(a)

(b)

(c)

Fig. 4. Surface morphology of fibers with different treatments (a) Raw, (b) Pre-treated, and (c) ZrO2-modified.

energy dispersive spectrometry (EDS) was performed on the hydration products precipitated on the embedded fibers surface.

3.2.1. Thermal stability analysis of embedded fibers

Thermogravimetric analysis was carried out to investigate the degradation of embedded hemp fibers caused by a mortar matrix throughout 28 d curing, not including the part wetting/drying cycles. This is because the embedded fibers due to the mineralized degradation, are stuck on the cementitious matrix and are difficult to separate.

Fig. 5 shows TG and DTG plots for the investigated degradation of fiber components under nitrogen atmospheres. TG Several distinct thermal degradations are observed on the DTG cures of the fibers: (1) the slight peak between 100 and 180 °C represented a loss of free water and combined water which comes from fibers structure and/or cement hydration products (C–S–H and ettringite). (2) a sharp peak was observed between 250 and 370 °C which corresponds to the degradation of hemicellulose and lignin, followed by cellulose [32,33]. (3) an evident shoulder observed around 400–550 °C for the embedded fibers in the cementitious matrix might be due to the decomposition of portlandite from the cement hydration products [34]. (4) Finally, the peak of about 650 °C corresponds to the residue decomposition of calcium carbonate residues on the extracted fiber surface.

Interestingly, prior to embedding, a small shoulder peak of the pre-treated fiber and the ZrO_2-modified fiber both occur at around 440 °C shown in Fig. 5(a). This is because this peak is the shoulder peak of cellulose degradation caused by the removal of the hemicellulose and extractives and then the improvement of the cellulose crystallinity index. The behavior is consistent with the DTG measurement of Almeida Melo Filho et al. [35]. In addition, the strong narrow peak of the ZrO_2 modified fibers non-embedded in cement matrix around 180–210 °C is observed. This is due to the removal of structural water molecules existing on the insulator zirconia, corresponding to M − OH bonding [36,37].

Based on the literature [18], a slightly small peak between 220 and 300 °C, which is associated with the degradation of hemi-cellulose, is observed in the DTG curves although the peak is not evident. It can also be seen from TG curves that pre-treated fibers have low mass loss no matter if embedded in the cement matrix. It is well known that the semi-crystalline cellulose components have better thermal stability than amorphous hemicellulose. After raw hemp fibers are alkali extracted, the semi-crystalline cellulose amount achieves a higher percentage of total components. Therefore, the pretreated step before fiber modification is quite necessary to improve thermal stability. More importantly, the embedded raw fibers have the highest rate of cellulose degradation at 3 and 7 days of aging, but aging to 28 days the embedded ZrO_2-modified fibers present the highest degradation rate. This indicates that the ZrO_2 modification delays its cellulose decomposition which implies the ZrO_2-modified fiber has better alkali resistance when subjected to the cementitious environment.
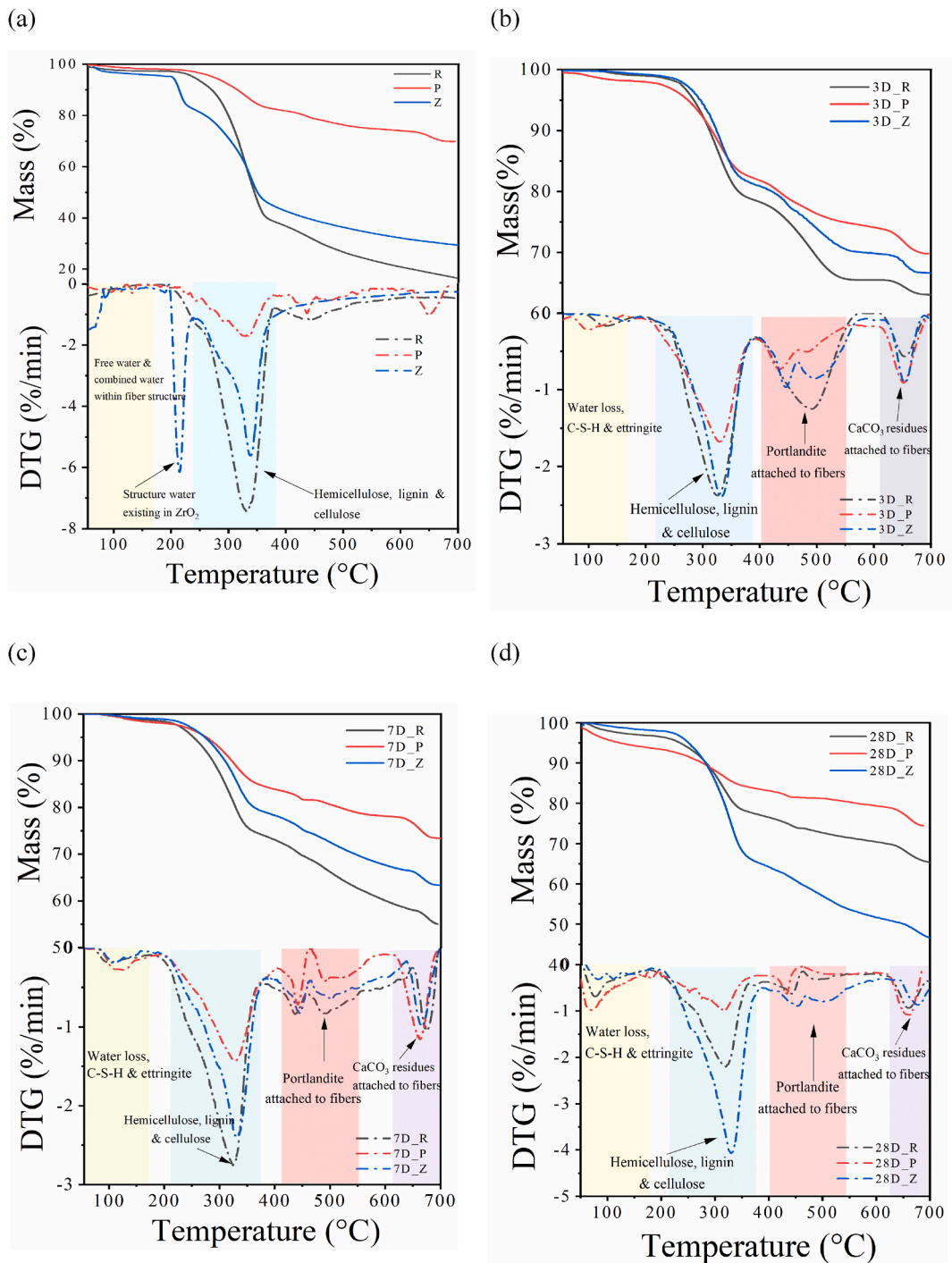
(a)

(b)

(c)

(d)

Fig. 5. Mass loss curves and DTG curves (b) of different treated fibers (R, Raw fibers; P, Pretreated fibers; Z, ZrO$_2$-modified fibers) before and after being subjected to different aging stages in cement mortars: (a) 0 d, (b) 3 d, (c) 7 d, and (d) 28 d.

Table 2 presents the change in thermal temperature representing the maximum rate of cellulose decomposition under different treatments and curing ages. After the initial 3 days of embedding in the cementitious matrix, the major shift to lower temperature of the DTG peaks occurred in both raw and pre-treated fibers, and a small shift for the ZrO$_2$-modified fibers. This indicates that cellulose is prone to undergo major degradation without the thermal insulation protection of ZrO$_2$ film. Subsequently, a considerable reduction in the DTG peak temperature of the pre-treated fibers at 28 days of embedded in the cement mortars. However, for the ZrO$_2$ modified fibers, the DTG peak at 7 days curing appears to keep the same level as the 3 days curing and then slightly shift to a lower temperature

Table 2
DTG peaks the temperature of cellulose of non-embedded/embedded hemp fibers under different curing stages.

	DTG peak temperature (°C)			
	Before	3 days	7 days	28 days
Raw	332	326	324	320
Pre-treated	336	328	328	316
ZrO$_2$-modified	338	332	332	330

at 28 days (330 °C). In general, a decrease in the peak temperature of cellulose was obtained for raw (3.6 %), pre-treated (6.0 %), and ZrO$_2$-modified fibers (2.3 %) during the 28 days of curing. This small peak shift suggests the ZrO$_2$ film acts as a thermal insulator protection to mitigate or even avoid the rapid degradation of cellulose. Also, the lower peak of DTG presented in the pre-treated fibers can be explained by the fact that cellulosic microfibrils' direct exposure to the cementitious alkali environment after the removal of extractives and hemicellulose, leading to the easy mineralization of surface microfibrils and then the decrease in the crystallinity degree of cellulose [18].

3.2.2. Hydration products analysis on the embedded fiber surface

To better understand the underlying effect of different treated fiber surfaces on cement hydration products, and assess their alkaline resistance, EDS analyses were conducted on the surface of embedded fibers to investigate any changes in the chemical composition before and after the wetting-drying cycling.

The effective element ratios of the materials were determined by two lines in Fig. 6 (a), Fig. 7 (a), Fig. 8 (a), Fig. 10 (a), and Fig. 11 (a). Results indicate that the dominant phases present on all fiber surfaces are typical of cement hydration products: CH, C–S–H, and AFm/AFt phase. The Al/Si ratio of C–S–H was determined by the slope of a dash-dot line, which is drawn through the points with the lowest Al/Ca ratio and represents mixed analyses of portlandite and C–S–H without AFm or ettringite. The solid line was drawn from the AFm element point (0, 0.5) and through the upper bound of the distribution of the Al/Ca atomic ratio. The range of Ca/Si ratios of C–S–H was roughly represented by the interior zone with dense bulk data points along the two lines. The discrete points with much lower Si/Ca ratio or higher Al/Ca ratio are due to deviations of EDS spectra caused by the pores, or thin C–S–H which is not sufficiently thick to minimize the contribution of adjacent phases [38].

From the below EDS, the Si/Ca in C–S–H was determined to be 0.56 ± 0.03 both before and after wetting-drying cycling. The determined ratio decreases within the range of previously reported data [39]. Richardson investigated that some Al^{+3} was substituted for Si^{+4} in the C–S–H. In addition, according to the linear relationship formula developed by Richardson and Groves, as is shown in Eq. (1) [40], a theoretical Al/Ca trace composition was estimated to be in the range from 0.04 to 0.06 based on the Si/Ca found in this work.

$$\frac{Si}{Ca} = 0.444 + 2.25 \frac{R}{Ca} \tag{1}$$

Where R is mainly Al (minor amount of Fe)

Bonen and Diamond [41] observed that the mean Al/Ca and S/Ca ratios were in the range from 0.034 to 0.066 and 0.037–0.06, respectively, and in C–S–H with Si/Ca approximately 0.43–0.48. Therefore, in this study, before wetting-drying cycling, Al/Ca and S/Ca were determined to be C–S–(A)-H phase and other phases like ettringite or monosulfate in the cement hydration products.

3.2.2.1. Prior to wetting/drying cycles. As seen in Fig. 6 (a), the Al/Ca and Si/Ca ratios of the hydration products precipitated on the ZrO$_2$-modified fiber surface are higher than the remaining two fibers after 3 days of curing. This appears to indicate that higher levels
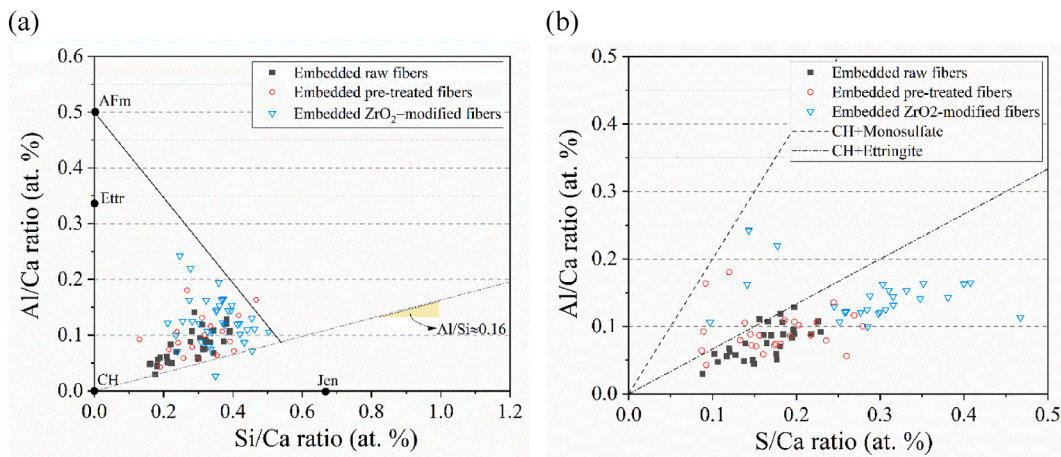

Fig. 6. Average Al/Ca versus Si/Ca molar ratios (a) and average Al/Ca versus S/Ca ratios (b) after 3 d curing, respectively.
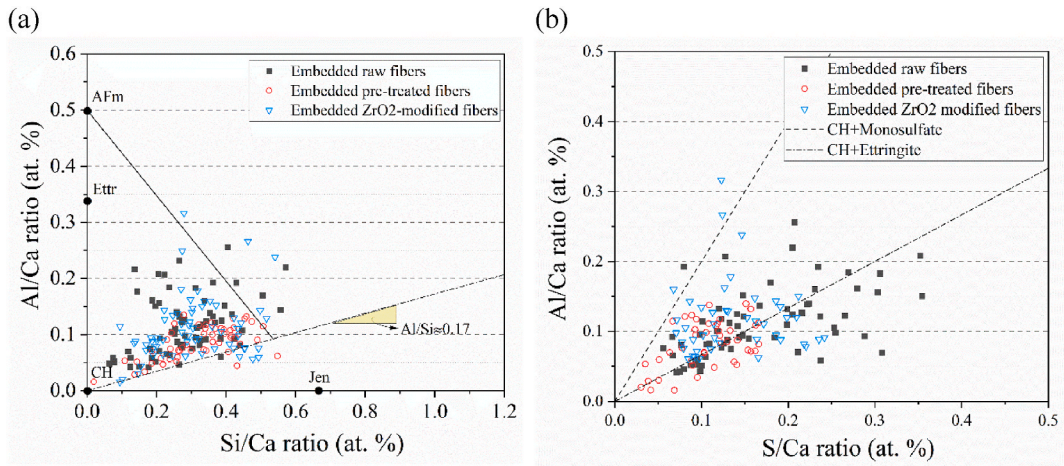
Fig. 7. Average Al/Ca versus Si/Ca molar ratios (a) and Average Al/Ca versus S/Ca ratios (b) after 7 d curing, respectively.
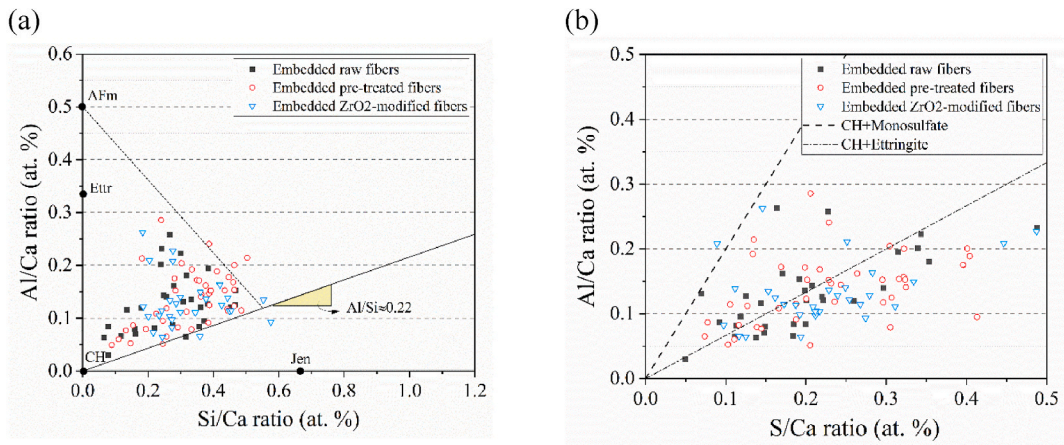

Fig. 8. Average Al/Ca versus Si/Ca molar ratios (a) and Average Al/Ca versus S/Ca (b) after 28 d curing, respectively.
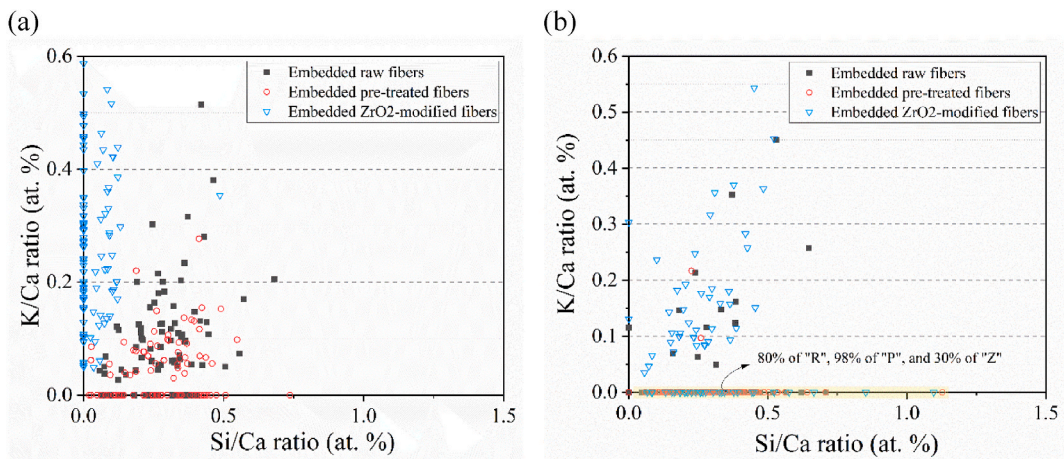

Fig. 9. Average K/Ca versus Si/Ca molar ratios after 7 d curing (a) and 28 d curing (b).

of the AFm/AFt phase and lower levels of portlandite are attached to the embedded fiber surface under the ZrO_2 modification. The calculated Ca/Si and Al/Si ratios of C–S–H on the ZrO_2-modified fiber surface are 2.65 ± 0.32 and 0.16, respectively, and the mean value of Ca/(Si + Al) is 2.28. Meanwhile, among the three treated fibers, the ZrO_2 treatment increased the relative amount of C–S–H phase precipitated on the fiber surfaces, as indicated by a relatively higher Si/Ca ratio. As for Fig. 6 (b), it appears that the major pots were concerned below the line of CH + ettringite mightly since the sulfate is loosely absorbed within the C–S–H. Furthermore, a relatively higher amount of CH appears on the embedded raw fiber and pre-treated fiber surface. This implies that these two embedded fibers are more easily attacked by the alkaline ions or mineralized by the portlandite from cement hydration products.

Based on the observation of Fig. 7 (a), there is no distinct difference in the Al/Ca and Si/Ca ratios for each type of fiber surface, only a slightly lower level of Al/Ca ratio in the embedded pre-treated fiber surface at 7 days of curing. The calculated Ca/Si and Al/Si ratios of C–S–H in all fiber surfaces are 3.17 ± 0.47 and 0.17, respectively. That means that the value of Ca/(Si + Al) is 2.71, which increases from 2.28 at 3 days due to the development of cement hydration. In addition, ettringite intermixed with more portlandite apparently precipitated on the pre-treated fiber surface, as indicated by the relatively lower Al/Ca and S/Ca ratios in Fig. 7 (b).

As seen in Fig. 7 (a), the range of Si/Ca ratio of C–S–H on the fiber surfaces at 28 d is similar to that at 7 days of curing, but the Al/Si ratio was increased up to 0.22. The calculated mean value of Ca/(Si + Al) is 2.60. That means, more SiO4 tetrahedrons of C–S(A)-H was replaced by AlO4⁻ tetrahedroa as the cement hydration developed. Besides, the S/Ca ratio range at 28 d is slightly higher than that at 7 days as illustrated in Fig. 8 (b). It is possibly related to the release of sulfate-containing liquid absorbed from the cement matrix, in the cavity of the embedded hemp fibers.

Fig. 9 illustrates the alkali content on the different treated fiber surfaces embedded in the cementitious matrix. The results obtained show that the major portion of Si/Ca ratio data focuses on below the value 0.5 and all K/Ca ratios are lower than 0.6 in both 7 d and 28 d of curing. As seen in Fig. 9 (a), all ZrO_2-modified fiber data fell on or around the K/Ca Y-axis with the lowest Si/Ca ratio while most pretreated fiber data distributed on the Si/Ca X-axis with a relatively higher Si/Ca ratio. This was probably related to the ion exchange due to the ionic species like ZrO^{2+} or Zr^{4+} existing in an alkali environment [42,43]. As also explained in Ref. [44] and Ref. [45], the alkali ions can be absorbed by the C–S–H gel. Thus, the C–S–H phase precipitated on the surface of the ZrO_2-modified fiber mainly exists in the formation of non-expansive C–K–S–H. At 28 d of curing, there was little difference in the Si/Ca ratio among the three fibers, but the K/Ca ratio in the raw fiber and pre-treated fiber almost fell to zero (Fig. 9 (b)). The reason for this phenomenon possibly is that the fiber surface without the barrier of ZrO_2 film is prone to absorb the K ions into the fiber lumen, especially for the pre-treated fibers, resulting in the K element not being detected by the EDS technique.

To summarize, during 28 d, the mineralization of the embedded pre-treated fiber is more serious compared to the other two embedded fibers. The hydration products precipitated on the pre-treated fiber surface are mainly portlandite intermixed with ettringite with increasing curing time. Whereas the hydration products on the surface of ZrO_2-modified fiber are mainly C–S–H phases, which exist in the form of non-expansive C–K–S–H.

3.2.2.2. After wetting/drying cycles. After 3 wetting-drying cycles, the embedded ZrO_2-modified fiber surface showed a significantly superior Al/Ca ratio and Si/Ca ratio (Fig. 10 (a)), and a lower S/Ca ratio (Fig. 10 (b)) compared to the other two fiber cases. This indicates that after ZrO_2 modification the production deposited on the embedded fiber surface mainly exists in the form of the alumina-rich phase (e.g., monosulfate). In general, the calculated Ca/Si ratio and Al/Si ratio of C–S–H on the fiber surfaces are 1.95 ± 0.22 and 0.11, respectively, and the mean value of Ca/(Si + Al) is 1.76, which notably decreased compared to those values prior to cycling. This could be possibly related to the transverting of more Ca sources into portlandite and calcite due to the curing under harsh environments (high temperature and cold water)

Up to 5 cycles, it can be evidently seen in Fig. 11 that the data of the embedded raw fibers are in the highest zone regarding both Al/Ca ratio and S/Ca but the relatively lower Si/Ca ratio. This phenomenon implies that more ettringite and C–S(A)-H phases in which the SiO4 tetrahedrons of C–S(A)-H were replaced by AlO4⁻ tetrahedrons, precipitated on the raw fiber surfaces. Compared to the raw fibers, both the pretreated fibers and ZrO_2-modified fibers have a relatively higher Si/Ca ratio as illustrated in Fig. 11 (a). This indicates that the SiO4 tetrahedrons of C–S–H were little or even not substituted by AlO4⁻ tetrahedrons for both fiber surfaces. In addition, the
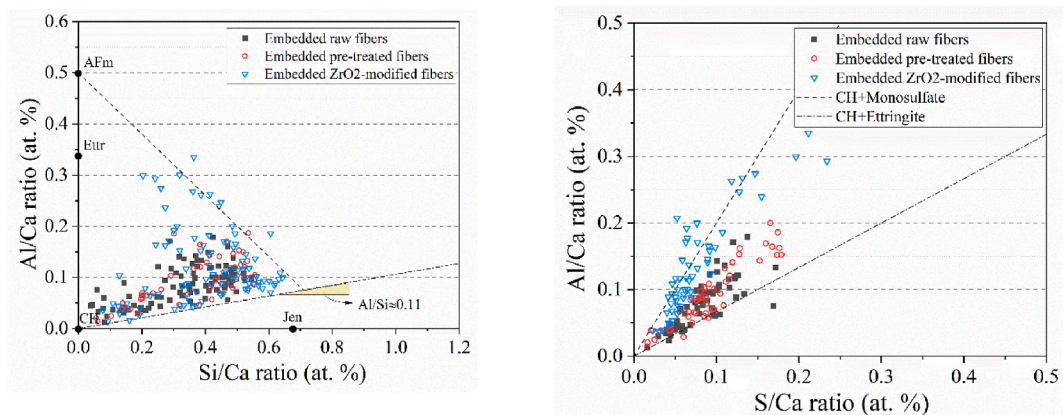

Fig. 10. Average Al/Ca versus Si/Ca molar ratios (a) and Average Al/Ca versus S/Ca (b) after 3 cycles, respectively.
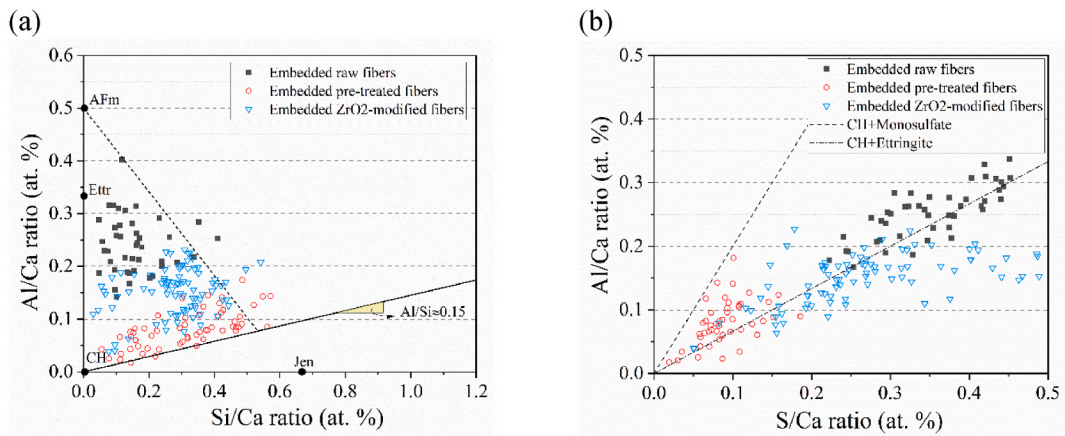
Fig. 11. Average Al/Ca versus Si/Ca molar ratios (a) and Average Al/Ca versus S/Ca (b) after 5 cycles, respectively.

lowest Al/Ca ratio and S/Ca ratio in Fig. 11 (b) indicates that more amount of portlandite or calcite and C–S–H phases exist on the pre-treated fiber surfaces. The phenomenon that increased the Al/Ca ratio and S/Ca ratio after ZrO_2 modification compared to the pre-treated fibers probably could be less amount of Ca existing on the phases on the fiber surfaces due to the alkali resistance of ZrO_2.

As a result, during wetting-drying cycles, the more ettringite and amorphous C–S(A)–H phases precipitated on the embedded raw fiber. Moreover, many SiO_4 tetrahedrons in C–S–H are substituted by AlO_4^- tetrahedrons. However, the pre-treated fibers still retain a significant amount of portlandite or calcite, along with partial C–S–H phases on their surface. In the case of ZrO_2-modified fibers, after the initial 3 cycles, predominant alumina-rich phases like monosulfate exist on their surface. Subsequently, as the wetting/drying continues, the less-Ca-contained phases precipitate on the fiber surface compared to the other embedded fibers. The resistance to alkali ions is attributed to the presence of the ZrO_2 film.

3.3. Effect of ZrO_2 modification on the durability of the composites

3.3.1. Mechanical strength of the composites

The mechanical strengths of HFRCCs are the most important criterion to assess the durability of the composites. Therefore, the compressive strength and flexural strength of the mortar composites reinforced with different treated fibers, after various curing days and wetting-drying cycles were investigated and the results were illustrated in Fig. 12.

It was evidently seen that the compressive strength (Fig. 12 (a)) and flexural strength (Fig. 12 (b)) increase with increasing curing time before the wetting-drying cycle. In addition, it is worth mentioning that the mortar composites reinforced with the fibers that underwent the pretreatment process (pretreated fibers and ZrO_2-modified fibers) have a somewhat higher flexural strength and compressive strength than the composites reinforced with raw fiber. This is possibly related to the difference in fiber stiffness with or without the pretreatment. The pretreatment can improve fiber flexibility, thus benefiting the flexural strength increase of the composites [46]. Meanwhile, this can result in more readily mechanical interlocking between the fiber and the matrix due to the rougher
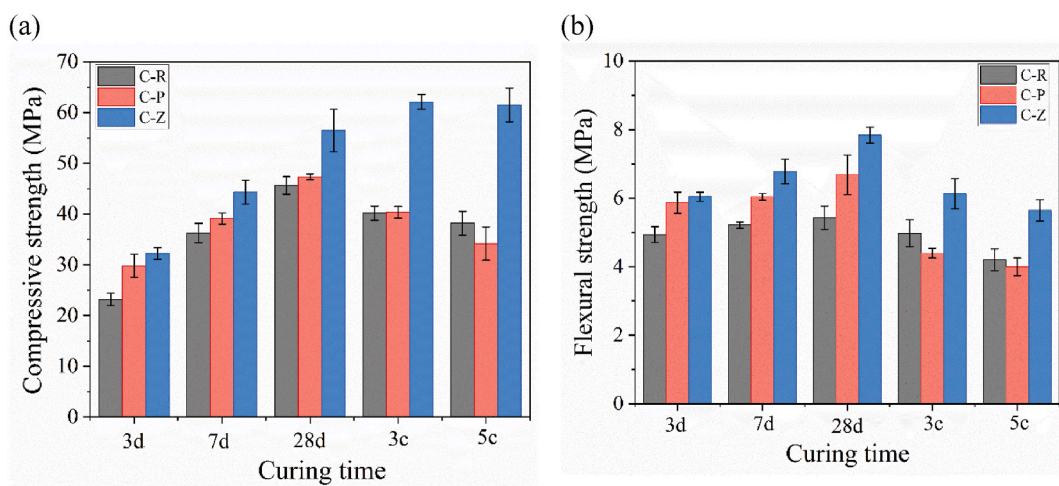

Fig. 12. Compressive strength (a) and flexural strength (b) of the mortar composites reinforced with hemp fibers, in which C–R, The mortar composites reinforced with raw hemp fibers; C–P, the mortar composites reinforced with pre-treated hemp fibers; C-Z, the mortar composites reinforced with ZrO2-modified hemp fibers.

surface, leading to sufficient compaction at high loading [47,48]. Further, the mortars reinforced with ZrO₂-modified fibers retain significantly higher mechanical strengths compared to those mortars reinforced with raw fiber or pre-treated fibers. That means ZrO₂-modified fibers can effectively improve the durability of their cement-based composites. This could be related to the interface compatibility between the fiber and the cement matrix, which will be discussed in the following section. As seen in Fig. 12 (a), the compressive strengths of C–R and C–P increased within the 28-d normal curing, followed by a considerable decrease during the wetting-drying cycles, a 16.3 % decrease for C–R and a 27.8 % decrease for C–P, respectively. However, for C-Z, the compressive strength continuously increased to 62.1 MPa until the third wetting-drying cycle and then only slightly reduced at the fifth cycle. It can be explained that the ZrO₂-modified fibers embedded into the cement matrix can provide an alkali-resistance film from the attack from the alkali cement hydration products as explained above. In terms of flexural strength shown in Fig. 12 (b), a similar trend, an increase within 28-d curing but a decrease in the period of the wetting-drying cycles, is observed for all the investigated composites. However, the degree of the trend is different, which is associated with fiber treatments. C-Z has an obvious increase in flexural strength within the initial 28-d curing and a slower reduction in the period of accelerated aging compared to C–R and C–P. By contrast, a sharp decrease in the initial three wetting-drying cycles was observed for C–P, which is attributed to the mineralization of the embedded pre-treated fibers, which has been explained in the section on thermal stability. Similar results are also reported in the literature [18]. Therefore, the ZrO₂ modification would be a quite potential approach to improve the durability of the NFRCCs.

3.3.2. Compatibility analysis of the composites

The interfacial bonding between fiber and cementitious matrix can directly influence the durability and mechanical strength of HFRCCs. Thus, in this work, it is necessary to evaluate the effect of ZrO₂ modification on the interface compatibility between the fibers and the cement matrix. According to the literature [49–51], hydration heat characteristics were widely used to assess the compatibility with cement for biomass fibers. The cross-compatibility index (CX) proposed by Sorin et al. [51] was employed as the compatibility indicator of HFRCCs in this study., as seen below in Eq. (2). In addition, to help understand Eq. (2), the typical heat hydration curves were introduced from our previous study (Fig. 13).

$$CX = \sqrt[3]{\frac{HR_{max}\, H_{3.5-24}\, t'_{max}}{HR'_{max}\, H'_{3.5-24}\, t_{max}}}$$
(2)

Where HR_{max} = maximum heat rate of HFRCCs (mW/g); HR'_{max} = maximum heat rate of neat cement paste (mW/g); $H_{3.5-24}$ = total heat (the area under heat rate curve) released by HFRCCs in 3.5–24 h interval (J/g); $H'_{3.5-24}$ = total heat (the area under heat rate curve) released by neat cement paste in 3.5–24 h interval (J/g); t_{max} = time to reach maximum heat rate of HFRCCs (h); t'_{max} = time to reach maximum heat rate of neat cement composite (h).

Table 3 presents the level of compatibility of the HFRCCs with different fibers (raw fiber, pre-treated fibers, and ZrO₂-modified fibers). According to the literature [51], three compatibility levels are divided: incompatibility level when the CX value is < 40, moderate compatibility level when the CX value is between 40 and 80, and compatibility level when the CX value is > 80. It was seen that all HFRCCs have high compatibility index values, which exceed 90 %. This can be attributed to the fact that hemp fibers have a relatively small amount of non-cellulosic substances (i.e. pectin, wax, and lignin) in comparison with other biomass fibers [52], which means less inhibition of the cement hydration. In comparison with C–R, both C–P and C-Z have relatively higher compatibility levels, which could be related to the removal of some extractives and sugars. Furthermore, for the case of C-Z with the highest compatibility level, there are several possible reasons associated with the synthesized ZrO₂ deposited on the fiber surface. Firstly, the ZrO₂ has a certain catalyze capacity which might accelerate the cement hydration reaction [30]; secondly, the fiber surface after ZrO₂ modification becomes quite rough (Fig. 4), which could benefit the mechanical interlocking of the interface in the composites [53] and
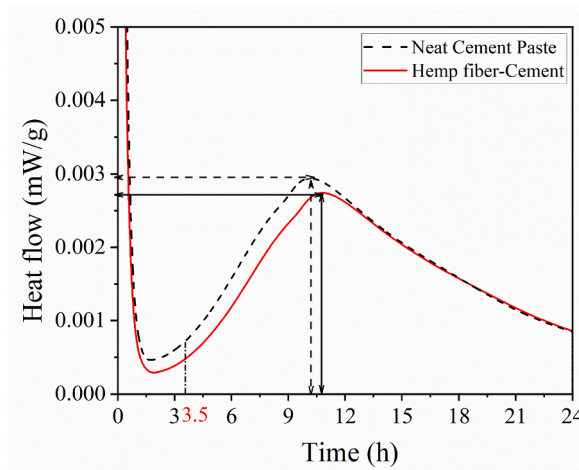

Fig. 13. Heat flow versus time for a neat cement paste (dashed curve) and a typical hemp fiber-cement (solid curve) which is depicted from the previous study.

Table 3
The cross-compatibility indexes of hemp fiber-reinforced cement composites.

	Hemp fiber-reinforced cement composites		
	C–R	C–P	C-Z
Cross compatibility indexes (CX)	90.1 %	94.2 %	99.8 %

increase the compatibility. Finally, the retardation effect on cement hydration reaction might be mitigated by the synthesized ZrO_2 layer that could prevent the fiber sugars components from directly contacting the cement matrix. Hence, the main conclusion is that ZrO_2 modification can benefit the compatibility increase between the fiber and cement matrix.

3.4. Alkali resistance behaviors of ZrO₂: alkali hydrolysis and mineralization

To compare the alkali resistance behaviors (alkaline hydrolysis and mineralization) of different treated fibers particularly ZrO_2-modified fibers, the strength stability of the fibers immersed in different alkaline mediums was studied. The following results will describe the peak tensile strength of different treated fibers immersed in different liquid environments (Water, NaOH solution, and saturation $Ca(OH)_2$ solution) as a function of the days. In this research, the pH value (pH ≈ 12.5) in the NaOH solution was kept the same value as that in the saturation $Ca(OH)_2$ solution to compare the alkali hydrolysis of the fibers (from attacking of hydroxide ions) [54] with the fiber mineralization caused by $Ca(OH)_2$ [55]. Besides, to minimize the influence of the water content of fibers on their tensile strength, the investigated fibers should be dried at 60 °C before the test every time according to Ref. [56]. Three different treated long fibers were used as investigated objects: raw fibers, pretreated fibers, and ZrO_2-modified fibers.

Fig. 14 shows the tensile strength of different treated fibers under various conditions. Before fogging, the an increase in the peak tensile strength after the pretreatment (acetone treatment and alkali treatment) compared to that of raw fibers (126.9 ± 4.3 MPa). This
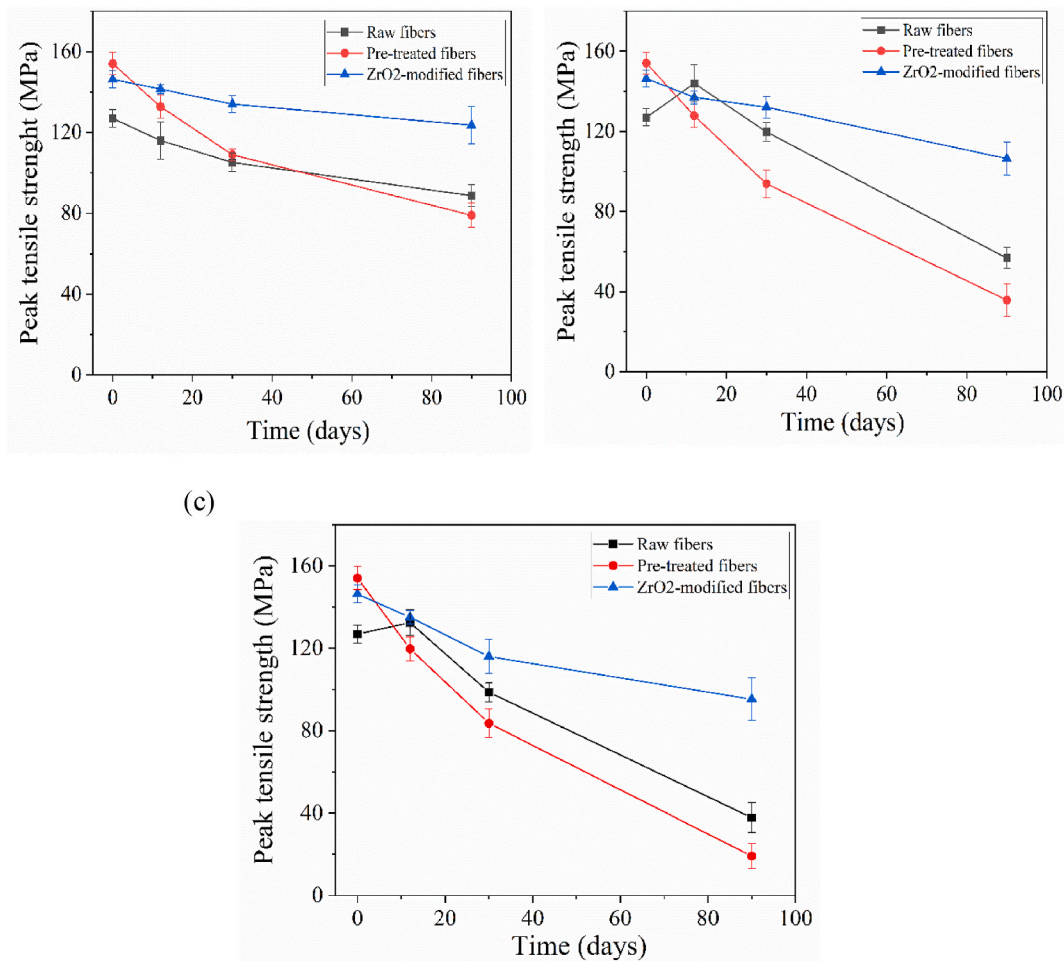

Fig. 14. Comparison of the peak tensile strength of untreated and treated hemp fibers (raw, pre-treated, and ZrO2-treated) before (0 days) and after being immersed in the water (a), NaOH solution (b), and saturation $Ca(OH)_2$ (c) for 12, 30 and 90 days.

was because the pretreatment process makes the fiber more flexible and softer by removing some non-cellulosic compounds. This result was also consistent with the literature [57,58]. However, a slight reduction (5 %) in the tensile strength after the ZrO_2 modification in comparison with that of pre-treated fibers. It is reasonably assumed that ZrO_2 particles attached to the fiber surface would restrict the movement of microfibril when the fiber is tensile, which is also confirmed by the SEM observation. Similar results are found in Ref. [59].

As expected, only a small decrease in tensile strength as the increase of the days was observed for the ZrO_2-modified fibers regardless of immersion in any medium (Fig. 14). In the water fogging environment depicted in Fig. 14 (a), the gradual decrease in the tensile peak of three different treated fibers may be related to microbiological action [60]. Meanwhile, the decreasing trend in ZrO_2-modified fibers is no remark compared to the other two fibers, which is attributed to the antibacterial property of synthesized ZrO_2 [61].

As seen in Fig. 14 (b) and Table 4, the pre-treated fibers experienced the most serious deterioration in the sodium hydroxide solution and decreased down to 76.8 % of their initial strength after 90 days, whereas the fibers after ZrO_2 modification had the slowest drop in tensile strength (27.3 %). Interestingly, it was observed that the peak tensile strength of raw fibers seems to be increased at the initial 3 days of storing in the alkali mediums. The reason is due to the removal of non-cellulosic substances from the fiber surface, which has already been mentioned above. In the case of the saturation calcium hydroxide environment (Fig. 14 (c)), the fiber degradation suffers more severely than that in the sodium hydroxide solution, reflected by the data of tensile strength downtrend. It is well-known that saturation $Ca(OH)_2$ additionally leads to fiber mineralization [62] except for the alkali hydrolysis, thus providing a more aggressive environment for the fiber. In comparison between the NaOH solution medium and saturation $Ca(OH)_2$ medium, it was clearly seen that the decrease in tensile strength caused by only the mineralization was not considerable compared to the alkali hydrolysis. In addition, it was observed that after 90 days raw and pre-treated fibers retained, respectively, 70.2 % and 87.6 % of their original strength which have been lost completely after 200 days. The flexibility of the air-dried fibers could be pulled apart fairly easily by finger force. For the ZrO_2-modified fibers, the loss of the original tensile strength of fibers was relatively less (retaining 65.1 %). Therefore, ZrO_2 modification not only could provide better alkali resistance behaviors (alkaline hydrolysis and mineralization).

4. Discussion

Durability tests on ZrO_2 modified fiber reinforced cement composites under accelerated aging conditions are an innovative measurement previously not focused on in the literature. Mechanical strength tests of the composites reinforced with different treated fibers (C–R, C–P, and C-Z) were conducted to evaluate their durability comparison. The mechanical strength behaviors of the composites can be well supported by the alkali resistance performances of embedded fibers and their compatibility with the cement matrix. In addition, the tensile strength measurement of different treated fibers (raw, pretreated, and ZrO_2-modified) in various controlled alkali solutions was carried out to compare alkali resistance behaviors: hydrolysis and mineralization. The results revealed the higher strengths of C-Z compared to C–R and C–P. It is caused by the presence of ZrO_2 which not only can prevent the degradation of fibers but also improve the interface compatibility between the fiber and the cement matrix. On the pre-treated fiber surface, according to EDS data, much portlandite and ettringite were observed which are prone to mineralization fibers, while the C–S–H phase is the main product precipitated on the ZrO_2-modified fiber which facilitates the interface adhesion (Fig. 15). Furthermore, the ZrO_2 modification exhibits greater resistance to the degradation caused by the alkali hydrolysis compared to the fiber mineralization.

The analyzed literature did not conduct the durability test on ZrO_2-modified reinforced cement composites under accelerated aging conditions. Boulos et al. [30] tested the mechanical strength of the composites reinforced with different treated fabrics within 90 days under normal conditions. The strength results of ZrO_2-treated fabric-reinforced cement composites were higher than untreated and pre-treated specimens. Nevertheless, the literature confirmed the alkali resistance effect of ZrO_2-treated fabrics and good interfacial adhesion to the matrix.

The literature [18,30] demonstrated that the use of ZrO_2 can effectively reduce the degradation of natural fibers in cementitious materials by its resistance behaviors. However, without comparing the resistance of ZrO_2 to alkali hydrolysis and mineralization, it is difficult to fundamentally explain the alkali resistance behaviors in the cement matrix.

In some literature [60,63,64], the comparison of alkali hydrolysis resistance and the mineralization resistance of natural fibers was determined based on their strength loss immersing into the NaOH and $Ca(OH)_2$ solutions, respectively. The results show the strength loss of fibers in the $Ca(OH)_2$ solution is more severe than that in the NaOH solution. This is mainly attributed to the crystallization of lime in the fiber lumen, voids, and walls in addition to alkaline hydrolysis. As expected, the above deliberations prove the alkaline resistance comparisons of the unmodified fibers in this study (Table 3). However, there is no statement about the alkaline resistance comparisons of the ZrO_2-modified fibers. In light of this, the tensile strength measurement of the ZrO2-modified fibers after immersing in various alkali mediums, was carried out in this work. When the ZrO_2-modified fibers suffered in the NaOH solution, the OH^- attack from the solution was effectively inhibited by forming a stable hydrated layer on the fiber surface due to the presence of ZrO_2 [65]. On the other hand, when exposed to $Ca(OH)_2$ solution, the strength loss of three fibers only caused by the mineralization was smaller than that caused by the alkali hydrolysis. This is because the fiber mineralization resulted from only $Ca(OH)_2$ here, rather than the complex cement hydration products ($Ca(OH)_2$, ettringite, and monosulfate) [62]. It is worth noting that only considering the strength loss caused by the mineralization, the degradation of ZrO_2-modified fibers is smaller compared to those of the other two treated fibers. This could be related to the formed ZrO_2 hydrated layer with selective permeability which is a certain resistance to the migration of (OH-, Ca^{2+}, and $Ca(OH)_2$) to the inner structure of the fibers, meaning the mitigated degradation process. Therefore, ZrO_2 modification not only could provide better resistance to alkali hydrolysis of fibers but also a certain extent alleviate the fiber mineralization.

In this study, an innovative fogging setup is designed to compare the alkali resistance behaviors mentioned above. If the modified/

Table 4
Strength loss of different treated fibers suffering in various alkali mediums after 90 d.

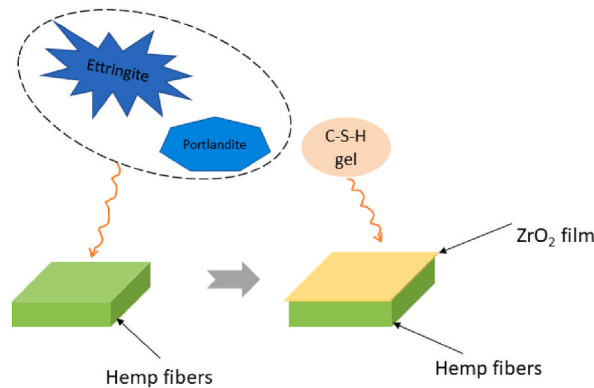|		Water	NaOH	Ca(OH)$_2$
Strength loss (%)	Raw	30.0	55.3	70.2
	Pre-treated	48.7	76.8	87.6
	ZrO$_2$ modified	15.6	27.3	34.9

Fig. 15. The schematic of cement hydration products precipitated on the surfaces of unmodified and modified fibers.

coated fibers were long-term immersed in the solutions, the modified/coated layer would be prone to be detached, affecting the experimental accuracy. Therefore, the common experimental setup (directly immersed fibers into various alkali solutions) used in the literature [60,63,64], is not suitable for modified/coated fibers. On the other hand, the fogging solution in the setup of this work avoids the problem of the peel-off of modified/coated layers from the fiber surfaces.

To sum up, ZrO$_2$-modified fibers reinforced cement composites, even under accelerated aging conditions, could efficiently improve durability due to their high alkali resistance performances and good interfacial adhesion to cement matrix. The use of NFRCCs is a good alternative to the high-carbon footprint production of traditional mortar/concrete materials, offering environmental and economic advantages. The results of this study can accelerate the practical application of NFRCCs, in particular in outdoor environments.

In this study, the feasibility of using ZrO$_2$ modification to enhance the durability of the composites under wetting-drying cycles was proven. However, the correlation between this accelerating aging and practical weather environment requires further study.

5. Conclusion

This work aimed to investigate the durability of hemp fiber (raw, pretreated, and ZrO$_2$-modified) reinforced cement composites under accelerating aging conditions. Relevant mechanical properties and micro-analyses of the composites were deeply studied. The following findings are drawn.

(1) The pretreatment resulted in the decoloration of hemp fibers from dark brown to yellow mainly due to the removal of the non-cellulosic substances. Further, the modified fibers presented a white-yellow color and rough surface owing to the existing ZrO$_2$ film.

(2) The pretreatment and ZrO$_2$ modification of the fibers promoted their thermal stability because of improved cellulose crystallinity index after hemicellulose and partial cellulose amorphous area removal, and the presence of insulator ZrO$_2$ film.

(3) During the normal curing period, the mineralization of the pre-treated fibers embedded in cement suffers the most severely evidenced by the much portlandite and ettringite precipitated on their surfaces. Whereas the C–S–H phases are the main products precipitated on the ZrO$_2$-modified fiber.

(4) Compared to the other two untreated and pretreated-fiber reinforced cement composites, ZrO$_2$-modified fiber-reinforced cement composites under accelerated aging conditions still maintain the highest mechanical strength. Cross-compatibility index calculations have proven that the compatibility level is better for the mortars containing ZrO$_2$-modified fibers which support higher mechanical properties when hemp fibers are within the cement.

(5) The alkali resistance test has demonstrated that alkali hydrolysis results in more significant degradation of fibers compared to mineralization. Importantly, the ZrO$_2$ modification exhibits excellent alkali resistance, regardless of both hydrolysis and mineralization.

It is necessary to highlight that the ZrO$_2$ modification can effectively improve the durability of hemp fiber-reinforced cement composites even though the composites are cured under harsh environmental conditions and the related alkali resistance mechanism of ZrO$_2$ in the NFRCCs is revealed. We believe that these findings will help guide the practical application of NFRCCs. Nevertheless, it has to be mentioned that the current study still has some limitations the composites in this study have not yet been conducted into a

practical application to test and related application cost lacks calculation. Thus, in future research, it is necessary to investigate the feasibility of the practical application of ZrO_2-modified hemp fiber-reinforced cement composites and expand the range of target natural fibers to increase the widespread application of the composites.

CRediT authorship contribution statement

Helong Song: Data curation, Methodology, Writing – original draft. **Tao Liu:** Formal analysis, Writing – review & editing. **Florent Gauvin:** Supervision, Visualization, Writing – review & editing, Conceptualization. **H.J.H. Brouwers:** Resources, Writing – original draft.

Declaration of competing interest

The authors certify that they have no affiliations with or involvement in any organization or entity with any financial interest, or non-financial interest in the subject matter or materials discussed in this manuscript.

Data availability

Data will be made available on request.

Acknowledgments

References

[1] A. Balea, E. Fuente, M.C. Monte, Á. Blanco, C. Negro, Fiber Reinforced Cement Based Composites, Fiber Reinforced Composites, Elsevier, 2021, pp. 597–648, https://doi.org/10.1016/B978-0-12-821090-1.00019-3.

[2] J. Shi, B. Liu, S. Chu, Y. Zhang, Z. Zhang, K. Han, Recycling air-cooled blast furnace slag in fiber reinforced alkali-activated mortar, Powder Technol. 407 (2022) 117686, https://doi.org/10.1016/j.powtec.2022.117686.

[3] H.M. Hamada, J. Shi, M.S. Al Jawahery, A. Majdi, S.T. Yousif, G. Kaplan, Application of natural fibers in cement concrete: a critical review, Mater. Today Commun. (2023) 105833, https://doi.org/10.1016/j.mtcomm.2023.105833.

[4] A. Quiroga, V. Marzocchi, I. Rintoul, Influence of wood treatments on mechanical properties of wood–cement composites and of Populus Euroamericana wood fibers, Compos. B Eng. 84 (2016) 25–32, https://doi.org/10.1016/j.compositesb.2015.08.069.

[5] V. Puri, P. Chakrabortty, S. Majumdar, A review of low-cost housing technologies in India, Adv. Struct. Eng.: Materials Three (2015) 1943–1955, https://doi.org/10.1007/978-81-322-2187-6_150.

[6] H. Song, T. Liu, F. Gauvin, Enhancing the mechanical performance of green fiber cement composites: role of eco-friendly alkyl ketene dimer on surfaces of hemp fibers, J. Mater. Res. Technol. (2023), https://doi.org/10.1016/j.jmrt.2023.12.255.

[7] C. Zhou, L. Cai, Z. Chen, J. Li, Effect of kenaf fiber on mechanical properties of high-strength cement composites, Construct. Build. Mater. 263 (2020) 121007, https://doi.org/10.1016/j.conbuildmat.2020.121007.

[8] F. Kesikidou, M. Stefanidou, Natural fiber-reinforced mortars, J. Build. Eng. 25 (2019) 100786, https://doi.org/10.1016/j.jobe.2019.100786.

[9] C. Sawsen, K. Fouzia, B. Mohamed, G. Moussa, Optimizing the formulation of flax fiber-reinforced cement composites, Construct. Build. Mater. 54 (2014) 659–664, https://doi.org/10.1016/j.conbuildmat.2013.12.038.

[10] B. Çomak, A. Bideci, Ö.S. Bideci, Effects of hemp fibers on characteristics of cement-based mortar, Construct. Build. Mater. 169 (2018) 794–799, https://doi.org/10.1016/j.conbuildmat.2018.03.029.

[11] H. Song, T. Liu, F. Gauvin, H. Brouwers, Improving the interface compatibility and mechanical performances of the cementitious composites by low-cost alkyl ketene dimer modified fibers, Construct. Build. Mater. 395 (2023) 132186, https://doi.org/10.1016/j.conbuildmat.2023.132186.

[12] R. De Gutiérrez, L. Diaz, S. Delvasto, Effect of pozzolans on the performance of fiber-reinforced mortars, Cement Concr. Compos. 27 (5) (2005) 593–598, https://doi.org/10.1016/j.cemconcomp.2004.09.010.

[13] J. Wei, C. Meyer, Utilization of rice husk ash in green natural fiber-reinforced cement composites: mitigating degradation of sisal fiber, Cement Concr. Res. 81 (2016) 94–111, https://doi.org/10.1016/j.cemconres.2015.12.001.

[14] Y. Ban, W. Zhi, M. Fei, W. Liu, D. Yu, T. Fu, R. Qiu, Preparation and performance of cement mortar reinforced by modified bamboo fibers, Polymers 12 (11) (2020) 2650, https://doi.org/10.3390/polym12112650.

[15] J.E. Mejia-Ballesteros, L. Rodier, R. Filomeno, H. Savastano Jr., J. Fiorelli, M.F. Rojas, Influence of the fiber treatment and matrix modification on the durability of eucalyptus fiber reinforced composites, Cement Concr. Compos. 124 (2021) 104280, https://doi.org/10.1016/j.cemconcomp.2021.104280.

[16] B. Zukowski, E.R.F. dos Santos, Y.G. dos Santos Mendonça, F. de Andrade Silva, R.D. Toledo Filho, The durability of SHCC with alkali-treated curaua fiber exposed to natural weathering, Cement Concr. Compos. 94 (2018) 116–125, https://doi.org/10.1016/j.cemconcomp.2018.09.002.

[17] G.H.D. Tonoli, M.N. Belgacem, G. Siqueira, J. Bras, H. Savastano Jr., F.R. Lahr, Processing and dimensional changes of cement based composites reinforced with surface-treated cellulose fibers, Cement Concr. Compos. 37 (2013) 68–75, https://doi.org/10.1016/j.cemconcomp.2012.12.004.

[18] L. Boulos, M.R. Foruzanmehr, A. Tagnit-Hamou, M. Robert, The effect of a zirconium dioxide sol-gel treatment on the durability of flax reinforcements in cementitious composites, Cement Concr. Res. 115 (2019) 105–115, https://doi.org/10.1016/j.cemconres.2018.10.004.

[19] M. Canovas, N. Selva, G. Kawiche, New economical solutions for improvement of durability of Portland cement mortars reinforced with sisal fibers, Mater. Struct. 25 (1992) 417–422, https://doi.org/10.1007/BF02472258.

[20] K. Bilba, M.-A. Arsene, Silane treatment of bagasse fiber for reinforcement of cementitious composites, Compos. Appl. Sci. Manuf. 39 (9) (2008) 1488–1495, https://doi.org/10.1016/j.compositesa.2008.05.013.

[21] K. Kamiya, S. Sakka, Y. Tatemichi, Preparation of glass fibres of the ZrO 2-SiO 2 and Na 2 O-ZrO 2-SiO 2 systems from metal alkoxides and their resistance to alkaline solution, J. Mater. Sci. 15 (1980) 1765–1771, https://doi.org/10.1007/BF00550596.

[22] T. Jung, R. Subramanian, Alkali resistance enhancement of basalt fibers by hydrated zirconia films formed by the sol-gel process, J. Mater. Res. 9 (4) (1994) 1006–1013, https://doi.org/10.1557/JMR.1994.1006.

[23] E.M. Salentijn, Q. Zhang, S. Amaducci, M. Yang, L.M. Trindade, New developments in fiber hemp (Cannabis sativa L.) breeding, Industrial crops and products 68 (2015) 32–41, https://doi.org/10.1016/j.indcrop.2014.08.011.

[24] C. Wang, Y. Zhang, H. Tan, X. Du, Non-calcined ZrO2 sol-coated hollow glass fiber membrane: preparation, microstructure, and dye separation, Ceram. Int. 47 (9) (2021) 12906–12915, https://doi.org/10.1016/j.ceramint.2021.01.153.

[25] J.L. Stapper, F. Gauvin, H. Brouwers, Influence of short-term degradation on coir in natural fibre-cement composites, Construct. Build. Mater. 306 (2021) 124906, https://doi.org/10.1016/j.conbuildmat.2021.124906.

[26] E.C.f. Standardization, EN, in: Methods of Testing Cement-Part 1: Determination of Strength, vols. 196–1, 2005.

[27] H. Wang, R. Postle, R. Kessler, W. Kessler, Removing pectin and lignin during chemical processing of hemp for textile applications, Textil. Res. J. 73 (8) (2003) 664–669, https://doi.org/10.1177/004051750307300802.

[28] R. Shanks, A. Hodzic, D. Ridderhof, Composites of poly (lactic acid) with flax fibers modified by interstitial polymerization, J. Appl. Polym. Sci. 99 (5) (2006) 2305–2313, https://doi.org/10.1002/app.22531.

[29] L. Boulos, M.R. Foruzanmehr, A. Tagnit-Hamou, S. Elkoun, M. Robert, Wetting analysis and surface characterization of flax fibers modified with zirconia by sol-gel method, Surf. Coating. Technol. 313 (2017) 407–416, https://doi.org/10.1016/j.surfcoat.2017.02.008.

[30] L. Boulos, M.R. Foruzanmehr, M. Robert, Evolution of the interfacial transition zone and the degradation mechanism of zirconia treated flax fabric reinforced cementitious composites, Construct. Build. Mater. 190 (2018) 120–130, https://doi.org/10.1016/j.conbuildmat.2018.09.104.

[31] S. Candamano, F. Crea, L. Coppola, P. De Luca, D. Coffetti, Influence of acrylic latex and pre-treated hemp fibers on cement-based mortar properties, Construct. Build. Mater. 273 (2021), https://doi.org/10.1016/j.conbuildmat.2020.121720.

[32] A.K. Both, D. Choudhry, C.L. Cheung, Valorization of hemp fibers into biocomposites via one-step pectin-based green fabrication process, J. Appl. Polym. Sci. 140 (10) (2023) e53586, https://doi.org/10.1002/app.53586.

[33] J.T. Mhlongo, Y. Nuapia, B. Tlhaole, O.T. Mahlangu, A. Etale, Optimization of hemp bast microfiber production using response surface modeling, Processes 10 (6) (2022) 1150, https://doi.org/10.3390/pr10061150.

[34] A. Hakamy, F. Shaikh, I.M. Low, Thermal and mechanical properties of hemp fabric-reinforced nano clay–cement nanocomposites, J. Mater. Sci. 49 (2014) 1684–1694, https://doi.org/10.1007/s10853-013-7853-0.

[35] J. de Almeida Melo Filho, F. de Andrade Silva, R.D. Toledo Filho, Degradation kinetics and aging mechanisms on sisal fiber cement composite systems, Cement Concr. Compos. 40 (2013) 30–39, https://doi.org/10.1016/j.cemconcomp.2013.04.003.

[36] D. Sarkar, D. Mohapatra, S. Ray, S. Bhattacharyya, S. Adak, N. Mitra, Synthesis and characterization of sol–gel derived ZrO2 doped Al2O3 nanopowder, Ceram. Int. 33 (7) (2007) 1275–1282, https://doi.org/10.1016/j.ceramint.2006.05.002.

[37] J. Liao, D. Zhou, B. Yang, R. Liu, Q. Zhang, Sol–gel preparation and photoluminescence properties of tetragonal ZrO2: Y3+, Eu3+ nano phosphors, Opt. Mater. 35 (2) (2012) 274–279, https://doi.org/10.1016/j.optmat.2012.08.016.

[38] F. Deschner, F. Winnefeld, B. Lothenbach, S. Seufert, P. Schwesig, S. Dittrich, F. Goetz-Neunhoeffer, J. Neubauer, Hydration of Portland cement with high replacement by siliceous fly ash, Cement Concr. Res. 42 (10) (2012) 1389–1400, https://doi.org/10.1016/j.cemconres.2012.06.009.

[39] H.F. Taylor, Cement Chemistry, Thomas Telford London, 1997, https://doi.org/10.1680/cc.25929.

[40] I. Richardson, G. Groves, The incorporation of minor and trace elements into calcium silicate hydrate (C–S–H) gel in hardened cement pastes, Cement Concr. Res. 23 (1) (1993) 131–138, https://doi.org/10.1016/0008-8846(93)90143-W.

[41] D. Bonen, S. Diamond, Interpretation of compositional patterns found by quantitative energy dispersive X-ray analysis for cement paste constituents, J. Am. Ceram. Soc. 77 (7) (1994) 1875–1882, https://doi.org/10.1111/j.1151-2916.1994.tb07065.x.

[42] A.J. Connelly, K.P. Travis, R.J. Hand, N.C. Hyatt, E. Maddrell, Composition–structure relationships in simplified nuclear waste glasses: 2. The effect of ZrO2 additions, J. Am. Ceram. Soc. 94 (1) (2011) 137–144, https://doi.org/10.1111/j.1551-2916.2010.04036.x.

[43] A. Paul, Chemical durability of glasses; a thermodynamic approach, J. Mater. Sci. 12 (1977) 2246–2268, https://doi.org/10.1007/BF00552247.

[44] B. Mohr, J. Biernacki, K. Kurtis, Supplementary cementitious materials for mitigating degradation of kraft pulp fiber-cement composites, Cement Concr. Res. 37 (11) (2007) 1531–1543, https://doi.org/10.1016/j.cemconres.2007.08.001.

[45] Y. Zhang, Z. Yang, J. Jiang, Insight into ions adsorption at the CSH gel-aqueous electrolyte interface: from atomic-scale mechanism to macroscopic phenomena, Construct. Build. Mater. 321 (2022) 126179, https://doi.org/10.1016/j.conbuildmat.2021.126179.

[46] X. An, R. Zhang, L. Liu, J. Yang, Z. Tian, G. Yang, H. Cao, Z. Cheng, Y. Ni, H. Liu, Ozone pretreatment facilitating cellulase hydrolysis of unbleached bamboo pulp for improved fiber flexibility, Ind. Crop. Prod. 178 (2022) 114577, https://doi.org/10.1016/j.indcrop.2022.114577.

[47] J. Khedari, B. Suttisonk, N. Pratinthong, J. Hirunlabh, New lightweight composite construction materials with low thermal conductivity, Cement Concr. Compos. 23 (1) (2001) 65–70, https://doi.org/10.1016/S0958-9465(00)00072-X.

[48] A.B. Akinyemi, E.T. Omoniyi, G. Onuzulike, Effect of microwave-assisted alkali pretreatment and other pretreatment methods on some properties of bamboo fiber reinforced cement composites, Construct. Build. Mater. 245 (2020) 118405, https://doi.org/10.1016/j.conbuildmat.2020.118405.

[49] M. Hachmi, A. Moslemi, A. Campbell, A new technique to classify the compatibility of wood with cement, Wood Sci. Technol. 24 (4) (1990) 345–354, https://doi.org/10.1007/BF00227055.

[50] Z.W. Bin Na, Wood-cement compatibility review, Wood Res. 59 (5) (2014) 813–826.

[51] S.A. Pasca, I.D. Hartley, M.E. Reid, R.W. Thring, Evaluation of compatibility between beetle-killed lodgepole pine (pinus contorta var. Latifolia) wood with Portland cement, Materials 3 (12) (2010) 5311–5319, https://doi.org/10.3390/ma3125311.

[52] F. Ahmad, H.S. Choi, M.K. Park, A review: natural fiber composites selection in view of mechanical, light weight, and economic properties, Macromol. Mater. Eng. 300 (1) (2015) 10–24, https://doi.org/10.1002/mame.201400089.

[53] M.M. Camargo, E. Adefrs Taye, J.A. Roether, D. Tilahun Redda, A.R. Boccaccini, A review on natural fiber-reinforced geopolymer and cement-based composites, Materials 13 (20) (2020) 4603, https://doi.org/10.3390/ma13204603.

[54] J. Wei, C. Meyer, Degradation mechanisms of natural fiber in the matrix of cement composites, Cement Concr. Res. 73 (2015) 1–16, https://doi.org/10.1016/j.cemconres.2015.02.019.

[55] G. Ren, T. Chen, X. Gao, A. Su, Insights into thermal stability and interface bond performance of sisal fiber in ultra-high performance concrete under different curing conditions, Cement Concr. Compos. 137 (2023) 104910, https://doi.org/10.1016/j.cemconcomp.2022.104910.

[56] D. Gomes dos Santos, A. Barbosa de Lima, P. de Sousa Costa, The Effect of the Drying Temperature on the Moisture Removal and Mechanical Properties of Sisal Fibers, Defect, and Diffusion Forum, Trans Tech Publ, 2017, pp. 66–71. https://doi.org/10.4028/www.scientific.net/DDF.380.66.

[57] M. Cai, H. Takagi, A.N. Nakagaito, M. Katoh, T. Ueki, G.I. Waterhouse, Y. Li, Influence of alkali treatment on internal microstructure and tensile properties of abaca fibers, Ind. Crop. Prod. 65 (2015) 27–35, https://doi.org/10.1016/j.indcrop.2014.11.048.

[58] P. Saha, S. Manna, S.R. Chowdhury, R. Sen, D. Roy, B. Adhikari, Enhancement of tensile strength of lignocellulosic jute fibers by alkali-steam treatment, Bioresour. Technol. 101 (9) (2010) 3182–3187, https://doi.org/10.1016/j.biortech.2009.12.010.

[59] X. Wang, L. Dou, Z. Li, L. Yang, J. Yu, B. Ding, Flexible hierarchical ZrO2 nanoparticle-embedded SiO2 nanofibrous membrane as a versatile tool for efficient removal of phosphate, ACS Appl. Mater. Interfaces 8 (50) (2016) 34668–34676, https://doi.org/10.1021/acsami.6b11294.

[60] G. Ramakrishna, T. Sundararajan, Studies on the durability of natural fibers and the effect of corroded fibers on the strength of mortar, Cement Concr. Compos. 27 (5) (2005) 575–582, https://doi.org/10.1016/j.cemconcomp.2004.09.008.

[61] N. Tabassum, D. Kumar, D. Verma, R.A. Bohara, M. Singh, Zirconium oxide (ZrO2) nanoparticles from antibacterial activity to cytotoxicity: a next-generation of multifunctional nanoparticles, Mater. Today Commun. 26 (2021) 102156, https://doi.org/10.1016/j.mtcomm.2021.102156.

[62] V.D. Pizzol, L.M. Mendes, H. Savastano Jr., M. Frías, F. Davila, M.A. Cincotto, V.M. John, G.H.D. Tonoli, Mineralogical and microstructural changes promoted by accelerated carbonation and aging cycles of hybrid fiber–cement composites, Construct. Build. Mater. 68 (2014) 750–756, https://doi.org/10.1016/j.conbuildmat.2014.06.055.

[63] L. Zhao, S. Zhu, H. Wu, H. Liang, C. Liu, W. Liu, W. Zhou, Y. Song, The improved resistance against the degradation of sisal fibers under the environment of cement hydration by surface coating of graphene oxide (GO) based membranes, Construct. Build. Mater. 305 (2021) 124694, https://doi.org/10.1016/j. conbuildmat.2021.124694.

[64] R.D. Tolêdo Filho, K. Scrivener, G.L. England, K. Ghavami, Durability of alkali-sensitive sisal and coconut fibers in cement mortar composites, Cement Concr. Compos. 22 (2) (2000) 127–143, https://doi.org/10.1016/S0958-9465(99)00039-6.

[65] R. Simhan, Chemical durability of ZrO2 containing glasses, J. Non-Cryst. Solids 54 (3) (1983) 335–343, https://doi.org/10.1016/0022-3093(83)90074-1.